Evaluation of habitat distribution and human imprints around an insular open-pit, Gyali Island, Southeast Aegean Sea

Vasiliki M. Tzafaridi[a], Ivan Petsimeris[a], Thomas Hasiotis*[a]

[a]Department of Marine Sciences, University of the Aegean, University Hill, 81100, Mytilene, Greece

ABSTRACT

Gyali is a small volcanic island in the Dodecanese. The present study used a high resolution hydroacoustic dataset, validated by camera and sediment samples, in order to investigate the habitat distribution, to compare sonar and satellite information regarding the distribution of seagrass and to detect potential anthropogenic imprints in the marine environment due to the onshore extraction activities. The seafloor has an uneven morphology and is characterized by numerous fluid seepages probably of hydrothermal origin, either extended or isolated. Side scan sonar analysis revealed six reflectivity types corresponding to specific seafloor morphology and consistency. Those were attributed to five marine substrates/habitats: sand, rippled sand, gravel-rhodoliths, *P. oceanica*, and reefs/rocky relief. Evidence of locally intense hydrodynamics was also observed. Satellite data concerning the spatial extent of seagrass was compared with the sonar recorded distribution, revealing significant differences, with only 44% of the total area mapped using satellite data corresponding with seagrass mapped in the present study. Anthropogenic targets related to anchor and mooring scars (few of them running through seagrass meadows) and other debris were detected scattered on the seafloor, mainly to the east and south of the island. Yet, the overall appearance of the habitat distribution and the visual inspection findings did not suggest considerable pressures from the onshore mining activities, even though biodiversity and other environmental studies need also to be implemented to confirm this conclusion.

Keywords: Marine habitat mapping, *P. oceanica*, Satellite data, Geomorphology, Anthropogenic targets, Gyali Island

1. INTRODUCTION

Gyali Island is a small, uninhabited island, located between the islands of Kos and Nisyros in the Southeast Aegean Sea (Figure 1). The geological composition of the island consists of a thick layer of rhyolitic pumice to the south and rhyolitic lava formations to the north[1, 2]. Those rhyolitic units are separated by an isthmus of loose coastal deposits at the center of the island. Northwest of Nisyros lies a magma pocket which in the past had activated a tectonic discontinuity near the Mandraki fault (in Nisyros) leading to seepage of H_2S on Gyali Island[3]. The Gyali offshore area has not been studied extensively in the past and the data, though limited, concerns mostly offshore bathymetry, morphotectonics, and general stratigraphy and not the shallower marine environment and ecological features/habitats. Only Daskalopoulou et al.[4] studied the geochemistry of shallow water fluid leakages (<10 m depth) observed in three sandy areas to the west and north of the island, whereas Nomikou et al.[3], while surveying the seafloor morphology of the eastern Aegean volcanic arc, discovered biogenic assemblages locally blanketing the volcanic hard substrate and a loose rippled sedimentary cover at the eastern part of the island, using an ROV, however not reporting positions or depth distribution. Yet, shallow and inshore habitats around Gyali Island had never been the focus of any research, although the wider area belongs to the NATURA 2000 network (Figure 1), and two mining companies actively extract pumice and perlite in the area. Only Topouzelis et al.[5] present information regarding the distribution of seagrass, as part of an effort to map the seagrass meadows around the entire Greek coasts using object-based image analysis in Landsat-8 images and machine learning. Thus, this contribution aims (i) to investigate the shallow morphology around the island and aid knowledge on the distribution of marine habitats, (ii) to assess potential pressures and human imprints induced due to the onshore extraction activities and (iii) to evaluate and compare data obtained from Topouzelis et al.[5] with the seagrass distribution recorded by sonar data in the present study.

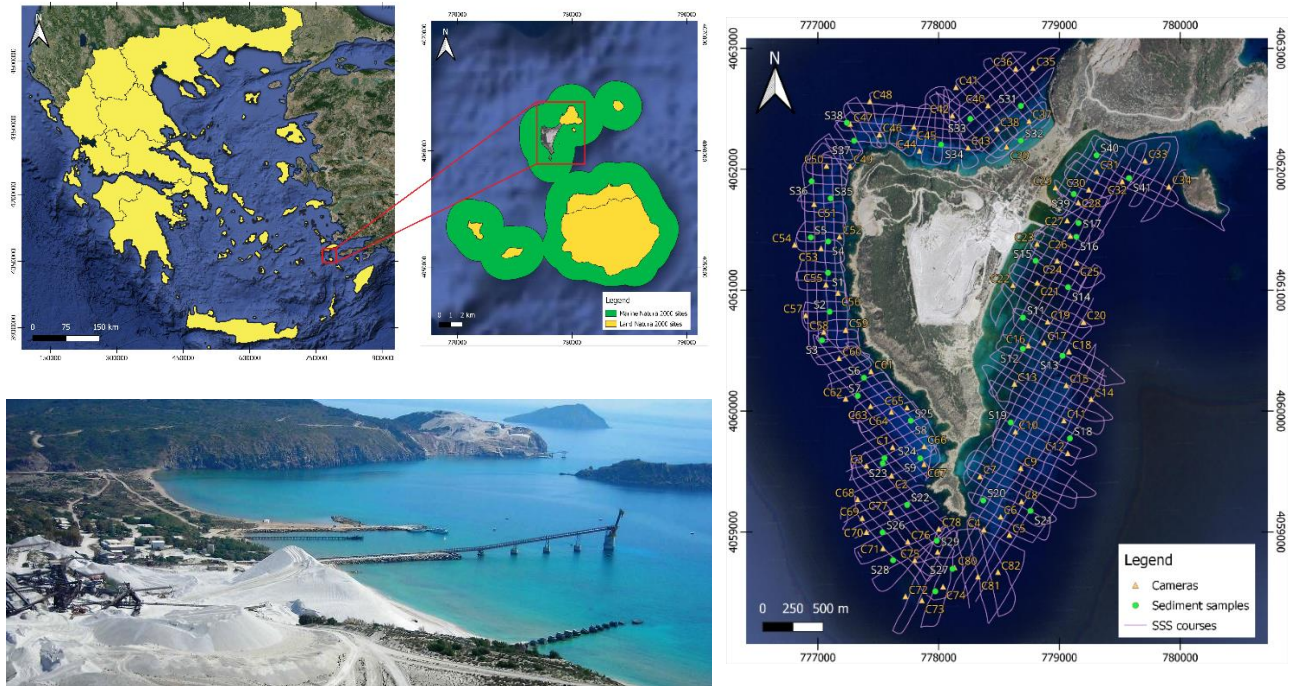*hasiotis@aegean.gr; phone +302251036829

Figure 1. Location of the study area (red boxes) also showing Marine and Land Natura 2000 sites around Gyali and Nisyros Islands (top left), and aerial photo of the extraction facilities on Gyali Island (bottom left). Filed observations and data collection locations (right).

2. METHODOLOGY

Data acquisition took place in September 2023, using (a) a high frequency hydrographic SonarMite v5 Echo-Sounder (Ohmex) (0.025 m depth accuracy - RMS) with GNSS RTK TopCon HiPer support (~0.5 m accuracy) and (b) a Humminbird Helix 10 multi-parametric sonar, being capable to simultaneously capture bathymetry (180-240 kHz) and map seafloor morphology operating in a side scan sonar (SSS) mode in 455 kHz. Both instruments were utilized to obtain bathymetric data. A dense grid of 58 parallel and 120 vertical survey lines was conducted, covering 6 km^2 (Figure 1). About 249,500 bathymetric points were recorded, filtered, and interpolated using a Multilevel B-Spline method for the creation of the bathymetric map in QGIS (Figure 2). The SSS images were processed and composed into a sonar mosaic (Figure 2) using the SonarWiz 7 software, while the seabed-habitat mapping was performed manually due to the morphological complexity of the area. The anthropogenic imprints were also mapped manually. A drop Go-Pro 4K camera was used for visual inspection of the seafloor and for ground-truthing of the SSS images through 82 videos. Also, 41 sediment samples were collected using a Van Veen grab. 37 out of 41 samples consisted mainly of coarse sediments (>0.0625 mm) and were analyzed by dry sieving according to Folk's[6] method. 4 samples consisted entirely of seagrass, and they were not analyzed. The Gradistat software[7] was used to calculate the samples' granulometric (statistic) parameters. Once the habitat mapping and ground-truthing were completed, the recorded seagrass distribution from the sonar data was compared with the available satellite data.

3. RESULTS

The bathymetric survey extended to a maximum depth of ~67 m (Figure 2). The seafloor morphology appeared uneven, with outcrops and one extensive reef to the south. To the east there is an extensive zone of low water depths with a micro-relief compared to the western side of the island where depths increase more abruptly. The slopes ranged from 0 to 80%, being lower (5-10%) in the shallow areas, also, off the two small beaches of the isthmus in the center of the island. Areas of hard substrate attain locally slopes higher than 45%. In general, between 5 and 15 m the slopes are smooth (~5%), from 15 to 50 m they increase abruptly up to 45%, with outcrops being up to 80% steep. Beyond 50 m the slopes increase more smoothly. The reef at the south extended between 5 and 20 m and displayed mean slopes between 5-15%.

A significant characteristic, which was detected in the bathymetric records, was the irregularly shaped and extensive strong reflections that are distributed from the bottom to the surface of the water column and were attributed to hydrothermal fluid venting. Several isolated and three extensive areas of seepage were recognized, between 5-55 m (Figure 2).
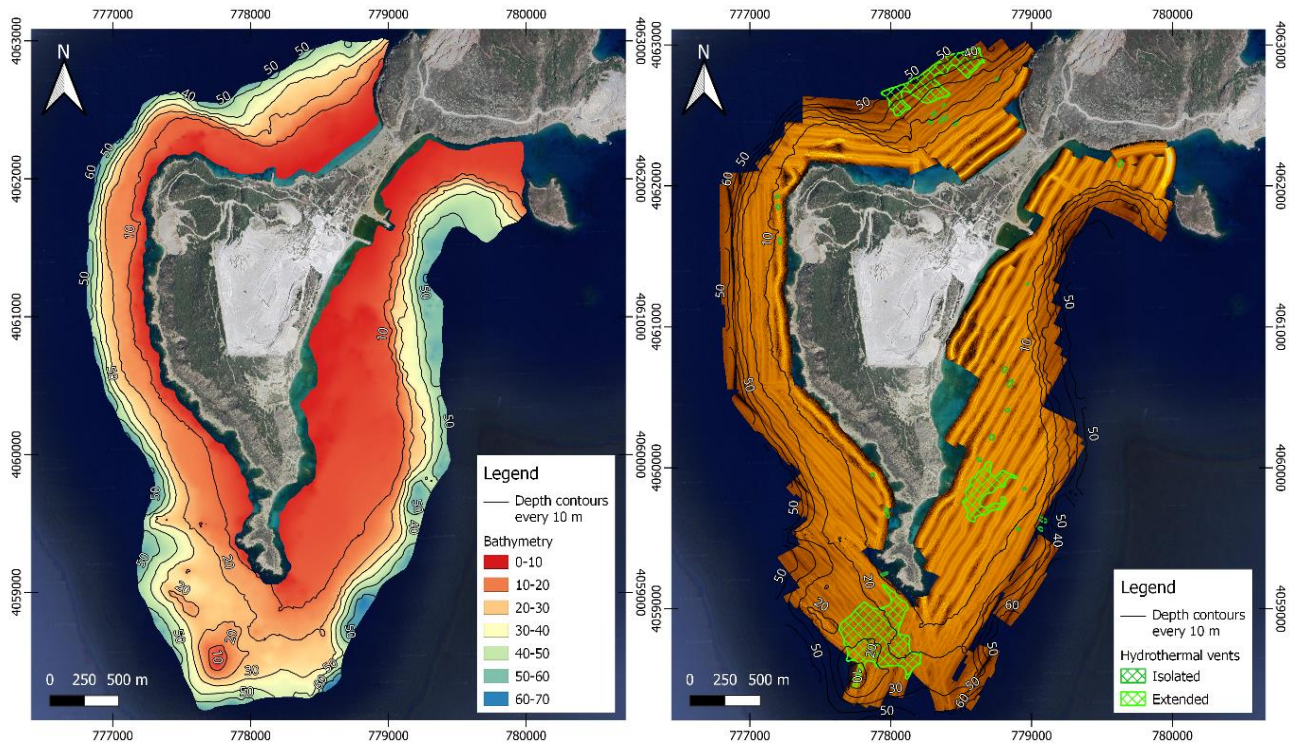

Figure 2. Bathymetry of the study area (left) and the side scan sonar mosaic with hydrothermal seepage areas (right).

Analysis and interpretation of the individual SSS images and the sonar mosaic revealed six main reflectivity types (RT), each corresponding to a different type of substrate or habitat (Table 1), as also validated by the camera observations and the sediment sampling:

RT 1a: Uniform medium reflectivity, corresponding to a smooth relief with loose sediments, mainly sand with varying percentages of gravel of various sizes (mean size (M): 0.23-4.81 mm). It occupies 2.6 km^2 (43.41% of the surveyed area), and it extends between depths of 0-55 m.

RT 1b: Similar to RT 1a but with higher reflectivity, corresponding to slightly coarser sand (M: 0.31 mm). It occupies 0.13 km^2 (2.09% of the surveyed area), extending between 0 and 25 m.

RT 1c: Similar to RT 1a but with lower reflectivity corresponding to finer sand (M: 0.16-0.25 mm). It occupies 0.29 km^2 (4.9% of the surveyed area), and it extends between depths of 5-40 m.

RT 2: Linear, rhythmic alternations of medium and low reflectivity due to the presence of sand ripples with few small gravels (M: 0.37-3.30 mm). This type takes up small, scattered areas mainly between other RT at depths ranging from 3 to 30 m. These bedforms are mainly attributed to wave activity in shallow waters, although currents may also play an important role. They occupy an area of 0.16 km^2 (2.75% of the studied area).
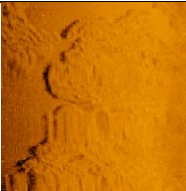
RT 3: Uniform low reflectivity, found mostly at greater depths (40 and 55 m) to the west of the island, as well as in limited areas at depths between 15-20 m and 20-40 m. The low backscatter demarcated the area to be separately mapped, but since the Humminbird SSS reflectivity cannot be considered reliable for bigger depths, videos and sediment samples were employed for ground-truthing and verified the existence of gravels and rhodoliths (M: 2.00-13.17 mm). It occupies 0.15 km^2 (2.43% of the surveyed area). The low reflectivity tone might also be due to the low density of the gravel (pumice).

RT 4: Medium to high reflectivity with irregular but relatively mild relief, sometimes followed by small shadows. It corresponds mainly to *P. oceanica* but also to other rarer seagrass types (i.e., *C. nodosa*), it is distributed between 5 and 35 m, and occupies 1.32 km^2 (21.96% of the studied area).

RT 5: Irregular alternations of medium to high reflectivity with intense relief usually followed by acoustic shadows of varying width and/or small areas of low reflectivity. This type corresponds to irregular rocky relief or to hard substrate with smoother relief, it extends almost all over the perimeter of the island, near the coast between 0 and 15 m, occupying 1.26 km^2 (21.05% of the surveyed area).

RT 6: Scattered targets of medium/high reflectivity followed by acoustic shadows in a medium reflectivity background. It corresponds to a transitional zone of scattered rocks in a sandy environment usually next to or close to RT 5. It extends between 1-5 m and occupies 0.09km^2 (1.41% of the surveyed area).

Table 1. Side scan sonar reflectivity types and camera snapshots of the seabed.

RT	SSS image	Camera snapshot	RT	SSS image	Camera snapshot
1a			3		
1b			4		
1c	Transition from 1b (lighter) to 1c (darker).		5		
2			6		

The wider mean size range of RT 1a is due to sand size variations but it may be also attributed to the lower specific gravity of pumice, which affects the way the acoustic energy is reflected and recorded. The placement of the sonar on the side of the boat, as well as the depth variations, may also affect the recorded reflectivity of similarly textured substrate, contributing to the wide mean size range obtained from sediment samples.

The observed sand ripples develop either almost parallel to the coast, indicating a wave origin, or almost vertical, probably indicating combining generation processes of waves and currents. In a particularly morphologically complex area to the south-southwest, significantly larger ripples were observed, indicating more complex dynamic processes.

The majority of the sediment samples that were analyzed contained biogenic fragments, whilst a few of them also seagrasses. The samples consisted exclusively of coarse sediments, gravel, and sand, and can be classified according to Folk[6] as medium gravel to fine grained sand (mean size: 0.16 to 13.17 mm). The gravel and sand content of the samples ranged from 0-100% and their spatial distribution was nearly complementary. According to the sediments' granulometric (statistic) parameters they ranged from well to poorly sorted (standard deviation: 1.22 to 3.64 μm) with the worst sorting occurring to the north. The sediments were strongly fine skewed to strongly coarse skewed (skewness: 0.54 to -1.25) and

very platykurtic to very leptokurtic (kurtosis: 0.32 to 2.34), indicating the mixing of various sediment sub-classes and of different origins (terrigenous and biogenic).

The observed RTs correspond to certain habitats (Figure 3) which can be categorized based on Directive 92/43/EEC (Network of Protected Areas NATURA 2000) (Table 2). Only RT 6 could not be categorized as it is a transitional type. Also, types 1110 and 1110-A extend from shallow to deep waters, instead of the shallow waters indicated by the Directive, thus they were also grouped under the code 119 which is devoted to soft sandy substrate.
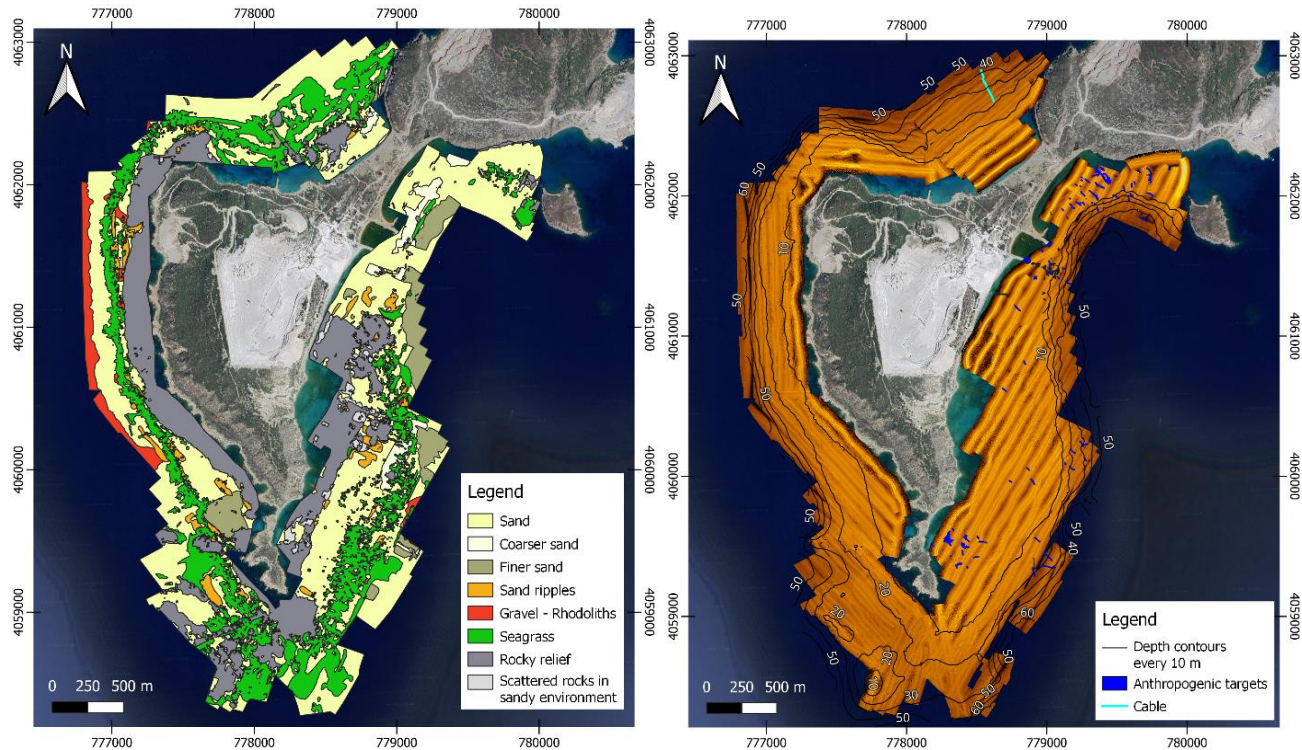

Figure 3. Habitat map over the studied area (left) and SSS mosaic showing location of anthropogenic targets (right).

Table 2. Reflectivity types and corresponding habitats of Directive 92/43/EEC (Network of Protected Areas NATURA 2000) found within the studied area.

RT	NATURA 2000 Code	Description	Depth Range (m)	Area	
				(km²)	(%)
1a, 1b, 1c	1110-A/119	Shallow subtype, Fine grained and well sorted sand biomes in shallow waters.	0-55	3.02	50.40
2	1110/119	Sand ripples constantly covered by sea water of small depth.	3-30	0.16	2.75
3	1110-B	Deep subtype, Rhodolithic fields: Coarse grained sand and gravel biomes and Coastal biogenic fragment biomes.	10-55	0.15	2.43
4	1120	Areas of marine vegetation with *Posidonia* (*Posidonion oceanicae*). *	5-35	1.32	21.96
5	1170-A	Shallow subtype of 1170, Shallow Reefs.	0-15	1.26	21.05

Cymodocea nodosa was also present locally.

Numerous scattered anthropogenic targets (mostly anchor scars, moorings, debris, construction bases, and a linear target) (Figure 4) were detected through the sonar images (mainly within RT 1 (Figure 3)) and were ground-truthed with camera

videos, mainly to the east and south, some of them near the extraction companies port facilities, in depths ranging from 5 to 35 m. The majority of the anchor scars were observed in the sandy substrate and/or between the rocky relief (Figure 4b). The construction bases of the port and the loading platform facilities were distinguished and inspected (Figure 4c). Three large containers connected by a chain, most likely acting as mooring, were also found between 35-40 m (Figure 4d). A linear trace with a length of 230 m was detected to the north, extending between 20 and 45 m water depth, corresponding to a submarine power or telecom cable connecting Gyali with Kos Island (Figure 4e). The overall appearance of the habitat distribution and the visual inspection did not suggest considerable pressures from the onshore mining activities; however, a small number of anchor scars ran through the seagrass meadows (Figure 4f), which may be attributed to fishing boats and yachts or bigger commercial ships.
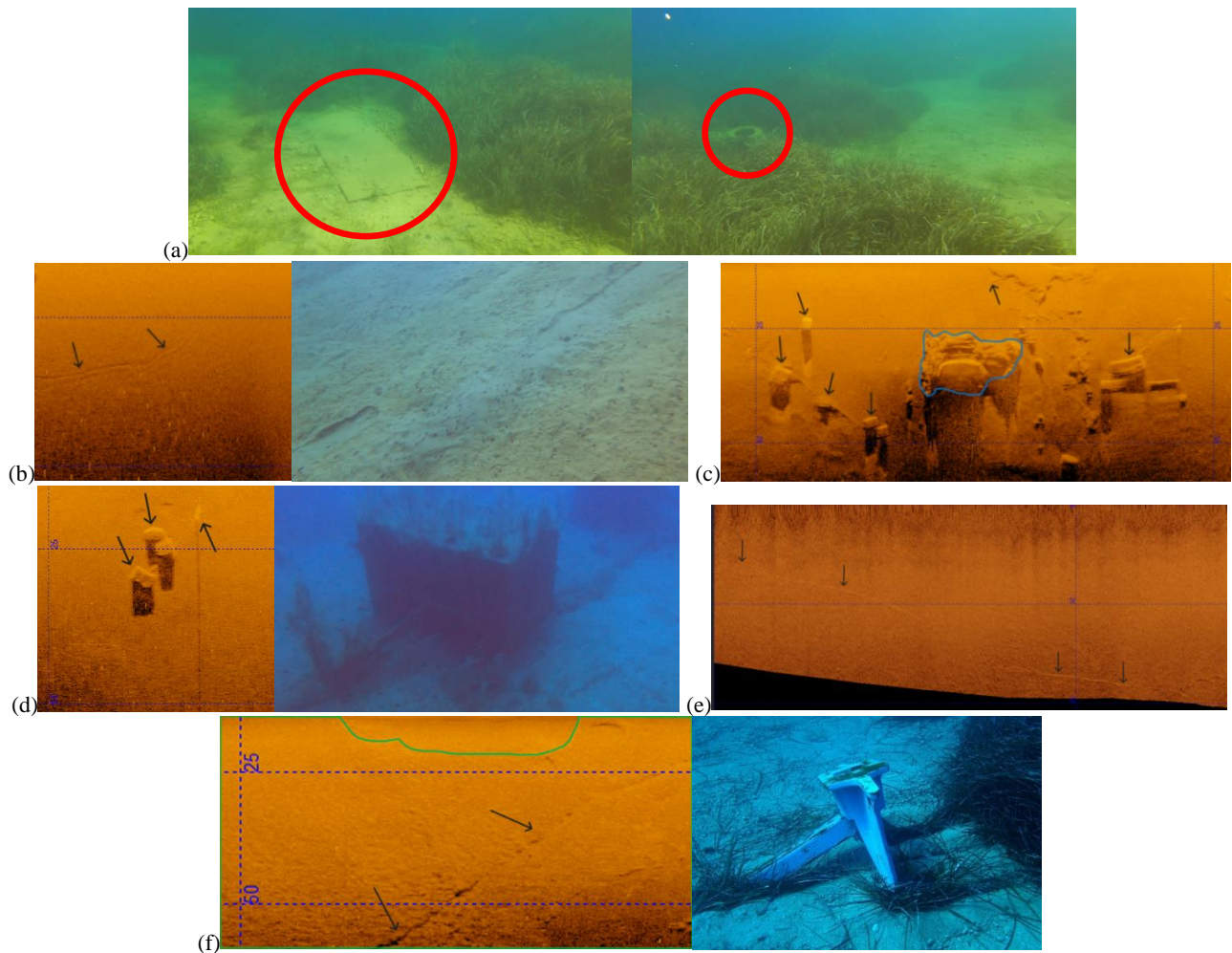

Figure 4. Examples of anthropogenic imprints (SSS images and camera photos) around Gyali Island. (a) A metallic plate and a tire littering the seafloor (red circles), (b) an anchor scar (black arrows) in a sandy substrate, (c) a construction foundation (blue outline) and various anthropogenic targets (black arrows), (d) moorings (black arrows), (e) the submarine cable trace (black arrows), and (f) an anchor scar (black arrows) and an abandoned anchor through *P. oceanica*. (scale: 25 m between blue dotted lines in the SSS images).

The seagrass meadows as detected in the sonar records in the present study occupied 1.32 km^2, while the meadows as observed by satellites[5] occupied 1.37 km^2. However, the common area recorded by the two methods (Figure 5) occupied 0.58 km^2, with only 44% of the total area mapped by satellite data corresponding to seagrass mapped by sonar data. The similarity observed in the size of the recorded areas is misleading, as the majority of the satellite classification was spatially misplaced. The classification conducted using satellite data appeared to encompass three types of errors:

(i) Inability to discern small seagrass patches or small pockets where seagrass was absent. This error is maybe related to the data's resolution which was obtained from Landsat-8 with a resolution of 30 m. To the north, south-southwest, and south-southeast of the island, wider areas were classified as seagrass, missing the pockets of sand amongst the meadows. Similarly, to the east a long but thin strip of seagrass was not recorded at all (Figure 5).

(ii) Mistaking other habitats, like the rocky relief, for seagrass meadows. Along the west coast the elongated strip of rocky relief in the shallow waters (Figure 3) was classified as seagrass. The same error occurred in the south where another wider area of rocky relief was also mistakenly classified.

(iii) Inability to detect the deeper limits of seagrass meadows. Especially to the north, an area of seagrass deeper than 20 m was not recorded at all.

Both methods were almost in agreement about the relative lack of seagrass in front of the port facilities.
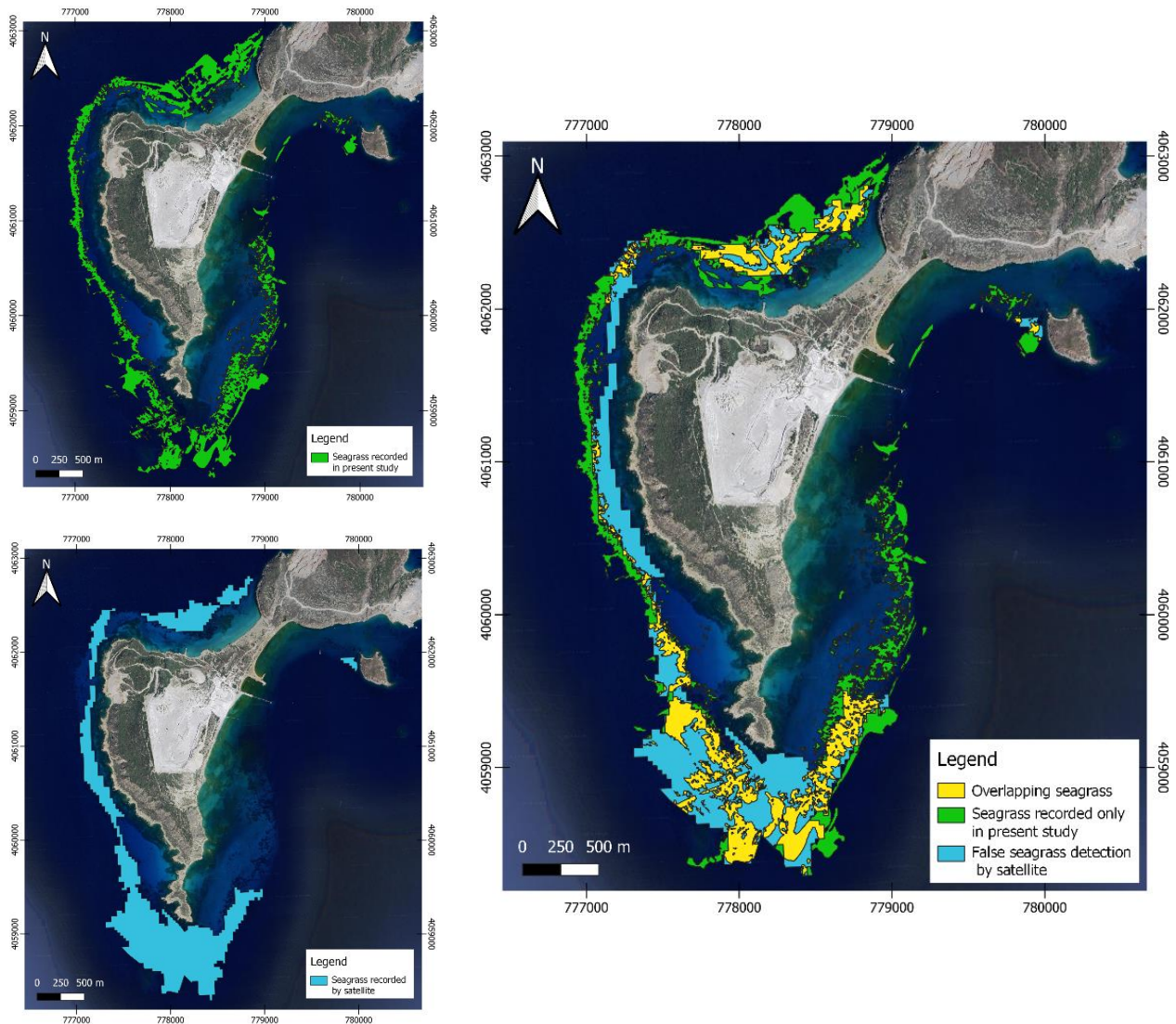

Figure 5. (left) Seagrass distribution of the present study (top), and according to the satellite data (bottom), and (right) differences in seagrass distribution according to the two classification methods and their overlap.

4. DISCUSSION AND CONCLUSIONS

Gyali Island is one of the very few open-pit uninhabited islands worldwide, where onshore extraction activities take place[8, 9, 10]. However, in none of the other open mining places, such as in Alaska[8] and Indonesia[9, 10], ecological or other

environmental studies have been reported. Similar studies are also missing for other coastal mines in operation, whilst few investigations report on the marine ecological and habitat status of big ports[11], at least in the Mediterranean Sea. Here, the distribution of marine habitats in the bigger part around Gyali, a Natura 2000 site but also an important insular open-pit, was studied in detail using common techniques for habitat mapping in shallow waters[12]. The surveyed area presents an uneven morphology with outcrops, reefs, areas with a sharp increase in slope, and shallow smooth areas, all of which are typical characteristics of a volcanic environment. Five main habitats were distinguished, which are sand and rippled sand (1110/119), reefs and rocky outcrops (1170-A), *P. oceanica* (1120) locally with pockets / small areas of *C. nodosa* and areas of rhodoliths and coarse-grained sediments (coarse sands to gravels) (1110-B). These are common habitats, which have been observed elsewhere, in shallow coastal areas, but also in the shelf of the Greek seas[13, 14]. *Posidonia oceanica* meadows and rhodolith fields are priority habitats protected by the EU Habitat Directive (92/43/EEC).

Submarine fluid seepages, either extended or isolated, most probably of a hydrothermal origin, were observed to occur mainly through rock outcrops, seagrass, and sand. The SSS images revealed the existence of sandy ripples attributed either to wave activity or locally to the intense hydrodynamic conditions also forced by the complex morphology (reefs, rocky outcrops, etc.).

Several anthropogenic targets were identified, some of which were ground-truthed by camera drops. In general, the visual inspection, apart from validating the interpretation of the SSS images, (i) confirmed the areas of fluid seepages, (ii) designated the quality (high clarity/visibility) of the water column, (iii) identified various targets of anthropogenic origin (construction foundations, moorings, anchor scars, litters, etc.). Litters on the seafloor are distributed on sand, in *P. oceanica* and near rocky outcrops. Although few of them, especially in front of the quarry dock, seem to be associated with the shipping activity there is no evidence regarding pressures induced due to the onshore mining works, even though biodiversity and other environmental studies need also to be implemented to confirm this conclusion.

Satellite imagery has been an important tool for widespread habitat mapping, especially in areas like the long Greek shoreline with numerous islands, where habitat mapping with hydroacoustic means is costly, time consuming, and difficult. However, satellite data presents relatively low resolution, depth limitations, and it requires extensive ground-truthing in order to validate the obtained data[15]. Ground-truthing is important in order to obtain reliable spatial data especially about protected and priority habitats like *P. oceanica* and coralligenous (rhodolithic) formations. In this study, the comparison of the seagrass distribution with that recorded by Topouzelis et al.[5] revealed significant differences, with only 44% of the total area mapped by satellite data corresponding with seagrass mapped in the current work. The errors observed exceeded 115% and ranged from inability to distinguish smaller targets to mistaking habitats like rocky relief/reefs for seagrass, as well as inability to discern the deeper limit of seagrass meadows. These significant errors and the small percentage of successful discrimination of seagrass show that classification through satellite data still presents many uncertainties and could not produce fully trustworthy results for this but also other coastal areas in the Greek seas with similar morphological and habitat characteristics, arising concerns but also dictating similar methodological evaluations to be adopted in order to achieve reliable outcomes.

REFERENCES

[1] Allen, S. R. and McPhie, J., "Water-settling and resedimentation of submarine rhyolitic pumice at Yali eastern Aegean Greece," J. Volcanol. Geotherm. Res. 95, 285–307 (2000). https://doi.org/10.1016/S0377-0273(99)00127-4

[2] Daskalopoulou, K., D'Alessandro, W., Longo, M., Pecoraino, G. and Calabrese, S., "Shallow Sea Gas Manifestations in the Aegean Sea (Greece) as Natural Analogs to Study Ocean Acidification: First Catalog and Geochemical Characterization," Front. Mar. Sci. 8:775247 (2022). https://doi.org/10.3389/fmars.2021.775247

[3] Nomikou, P., Papanikolaou, D., Alexandri, M., Sakellariou, D. and Rousaksi, G., "Submarine volcanoes along the Aegean volcanic arc," Tectonophysics, 597-598, 123-146 (2013). https://doi.org/10.1016/j.tecto.2012.10.001

[4] Daskalopoulou, K., Calabrese, S., Gagliano, A. L., Kyriakopoulos, K., Vigni, L. L., Longo, M., Pecoraino, G. and D'Alessandro, W., "Chemical characterization of the gases released at Gyali Island, Dodecanese, Greece and preliminary estimation of the CO2 output," It. J. Geosci. 140, 16–28 (2021). https://doi.org/10.3301/IJG.2020.18

[5] Topouzelis, K., Makri, D., Stoupas, N., Papakonstantinou, A. and Katsanevakis, S., "Seagrass mapping in Greek territorial waters using Landsat-8 satellite images," International Journal of Applied Earth Observation and Geoinformation, 67 (2018). https://doi.org/10.1016/j.jag.2017.12.013

[6] Folk, R., "Petrology of Sedimentary Rocks," HEMPHILL'S Drawer M. University Station, Austin, Texas, p.169 (1968).

[7] Blott, S. J. and Pye, K., "Gradistat: A Grain Size Distribution and Statistics Package for the Analysis of Unconsolidated Sediments," Earth Surf. Proc. Landf., 26, 1237-1248 (2001). https://doi.org/10.1002/esp.261

[8] Dahners, L. A., "Preliminary report on some pumice deposits, Augustine Island, Alaska," Territory of Alaska, Department of Mines (1947).

[9] Siti, F. and Yusuf, H., "Analisis Pengaruh Belanja Daerah Terhadap Pertumbuhan Product Domestic Regional Brutto (PDRB) Di Kabupaten Lombok Barat Tahun 2016-2019," Journal of Economics and Business, 6(2), pp. 1 – 27 (2020). https://doi.org/10.29303/ekonobis.v5i2.45

[10] Mutaqin, B. W., Lavigne, F., Sudrajat, Y., Handayani, L., Lahitte, P., Virmoux, C., Hiden, Hadmoko, D. S., Komorowski, J. C., Hananto, N. D., Wassmer, P., Hartono and Boillot-Airaksinen, K., "Landscape evolution on the eastern part of Lombok (Indonesia) related to the 1257 CE eruption of the Samalas Volcano," Geomorphology, 327 (2018). https://doi.org/10.1016/j.geomorph.2018.11.010

[11] Dimitriou, P., Chatzinikolaou, E. and Arvanitidis, C., "Ecological status assessment based on benthic macrofauna of three Mediterranean ports: comparisons across seasons, activities and regions," Marine Pollution Bulletin (2020). https://doi.org/10.1016/j.marpolbul.2020.110997

[12] Tecchiato, S., Buosi, C., Ibba, A., Del Deo, C., Parnum, I., O'Leary, M. and De Muro, S., "Geomorphological and sedimentological surrogates for the understanding of seagrass distribution within a temperate nearshore setting (Esperance Western Australia)," Geo-Marine Letters, 39, 249-264 (2019). https://doi.org/10.1007/s00367-019-00571-5

[13] Dimas, X., Fakiris, E., Christodoulou, D., Georgiou, N., Geraga, M., Papathanasiou, V., Orfanidis, S., Kotomatas, S. and Papatheodorou, G., "Marine priority habitat mapping in a Mediterranean conservation area (Gyaros, South Aegean) through multi-platform marine remote sensing techniques," Frontiers in Marine Science, 9, 953462 (2022). https://doi.org/10.3389/fmars.2022.953462

[14] Fakiris, E., Dimas, X., Giannakopoulos, V., Geraga, M., Koutsikopoulos, C., Ferentinos, G. and Papatheodorou, G., "Improved predictive modelling of coralligenous formations in the Greek Seas incorporating large-scale, presence–absence, hydroacoustic data and oceanographic variables," Frontiers in Marine Science, 10 (2023). https://doi.org/10.3389/fmars.2023.1117919

[15] Poursanidis, D., Topouzelis, K. and Chrysoulakis, N., "Mapping coastal marine habitats and delineating the deep limits of the Neptune's seagrass meadows using very high resolution Earth observation data," International Journal of Remote Sensing (2018). https://doi.org/10.1080/01431161.2018.1490974